Gz Enhanced Signal Transduction assaY (G$_Z$ESTY) for GPCR deorphanization

Luca Franchini, Joseph J. Porter, John D. Lueck, and Cesare Orlandi *

Department of Pharmacology and Physiology, University of Rochester Medical Center, Rochester, NY 14642, USA

 * Correspondence: cesare_orlandi@urmc.rochester.edu

Running title:

G$_Z$ESTY assay

1

Abstract

G protein-coupled receptors (GPCRs) are key pharmacological targets, yet many remain underutilized due to unknown activation mechanisms and ligands. Orphan GPCRs, lacking identified natural ligands, are a high priority for research, as identifying their ligands will aid in understanding their functions and potential as drug targets. Most GPCRs, including orphans, couple to $G_{i/o/z}$ family members, however current assays to detect their activation are limited, hindering ligand identification efforts.

We introduce G_ZESTY, a highly sensitive, cell-based assay developed in an easily deliverable format designed to study the pharmacology of $G_{i/o/z}$-coupled GPCRs and assist in deorphanization. We optimized assay conditions and developed an all-in-one vector employing novel cloning methods to ensure the correct expression ratio of G_ZESTY components. G_ZESTY successfully assessed activation of a library of ligand-activated GPCRs, detecting both full and partial agonism, as well as responses from endogenous GPCRs. Notably, with G_ZESTY we established the presence of endogenous ligands for GPR176 and GPR37 in brain extracts, validating its use in deorphanization efforts. This assay enhances the ability to find ligands for orphan GPCRs, expanding the toolkit for GPCR pharmacologists.

2

1. INTRODUCTION

In mammals, G Protein Coupled Receptors (GPCRs) are the largest family of cell surface receptors and are involved in a wide range of physiological and pathological processes[1,2]. Orphan GPCRs are those whose natural ligands have not yet been identified or agreed upon, making them difficult to study. Deorphanization, the process of identifying endogenous ligands for orphan GPCRs, is often achieved by analyzing receptor activation by candidate ligands in heterologous cell systems. These candidate ligands are selected based on their overlapping *in vivo* localization with a target GPCR, by isolation from tissue extracts that exert measurable physiological effects, or via screening of large libraries of endogenous compounds including small molecules, peptides, and lipids with a demonstrated biological activity[3-11]. Research that led to the deorphanization of the Glucagon-Like Peptide-1 (GLP1) receptor illustrates how identifying a GPCR's endogenous ligand can unlock new therapeutic opportunities. Initially discovered as a gut-derived hormone that enhances insulin secretion in response to elevated plasma glucose levels[12], GLP1 was found to bind to a putative receptor in the brain and pancreas[13,14]. This discovery led to the cloning of its receptor, a GPCR, in the early 1990s[15-17]. Since then, numerous GLP1 receptor agonists have been approved for treating type 2 diabetes mellitus and, more recently, for chronic weight management in adults with obesity[18-20].

A central challenge in the process of deorphanization is the choice of a measurable outcome of receptor activation. Cell-based assays exploiting various signaling properties and readouts have been developed, each with their own advantages and limitations. These assays measure proximal events such as heterotrimeric G protein dissociation[21-24] or β-arrestin recruitment[25,26]; they quantify the accumulation of second messengers[27-30]; or they utilize genetic reporters that depend on transcriptional regulation events initiated by GPCRs[31,32]. Further sets of assays are label-free and agnostic to the molecular mechanism leading to the change being measured[33,34]. All of these assays differ in sensitivity and time required to obtain a measurable signal. Most importantly, when studying orphan GPCRs, lack of information about G protein coupling profile or ability to recruit β-arrestins requires further considerations. To partially address this issue, we recently quantified the constitutive activity of several orphan GPCRs and showed that many are coupled to G proteins belonging to the $G_{i/o/z}$ family[35].

Here, we performed an in-depth optimization of a cell-based assay aimed at measuring $G_{i/o/z}$ coupled receptor activation. We demonstrated an improved sensitivity and the wide applicability of this assay that we named G_z Enhanced Signal Transduction assaY (G_zESTY). We generated and tested an all-in-one plasmid for the mammalian expression of each component required for

3

74   G_zESTY at the optimized ratio. Finally, we applied this assay to demonstrate the presence of

75   endogenous ligands for orphan receptors GPR176 and GPR37 in unfractionated mouse brain

76   extract.

77

78   **2. METHODS**

79   **2.1 Cell cultures and transfections**

80   HEK293T/17 cells were purchased from American Type Culture Collection (ATCC) and cultured

81   at 37°C and 5% CO_2 in Dulbecco's Modified Eagle's Medium (DMEM; Gibco, 10567-014)

82   supplemented with 10% fetal bovine serum (FBS; Biowest, S1520), Minimum Eagle's Medium

83   (MEM) non-essential amino acids (Gibco, 11140-050), sodium pyruvate (Gibco, 11360-070),

84   GlutaMAX (Gibco, 35050-061), and antibiotics (100 units/ml penicillin and 100 µg/ml

85   streptomycin; Gibco, 15140-122). 1×10^6 cells/well were seeded in 6-well plates in medium

86   without antibiotics. After 4 hours, cells were transfected using linear 25 kDa polyethylenimine

87   (PEI) (Polysciences; 23966) at a 1:3 ratio between total µg of DNA plasmid (2.5 µg) and µl of PEI

88   (7.5 µl). A pcDNA3.1 empty vector was used to normalize the amount of transfected DNA.

89   Charcoal-stripped FBS (S162C) and dialyzed FBS (347G18-D) were purchased from Biowest.

90   **2.2 DNA constructs and cloning**

91   Plasmids encoding Dopamine D2 Receptor (D2R), GABAB receptor subunits (GABBR1 and

92   GABBR2), α2-adrenergic receptor 2A (ADRA2A), µ-opioid receptor (MOR), δ-opioid receptor

93   (DOR), κ-opioid receptor (KOR) α2-adrenergic receptor 2B (ADRA2B), α2-adrenergic receptor

94   2C (ADRA2C), serotonin receptor 1B (5-HT1B), masGRK3CT-Nluc, PTX-S1, and $G\alpha_{oA}$ were

95   generous gifts from Dr. Kirill Martemyanov (UF Scripps Institute, FL). $G\beta_1$-Venus[156-239] and $G\gamma_2$-

96   Venus[1-155] were generous gifts from Dr. Nevin Lambert (Augusta University, GA) [22]. Codon-

97   optimized coding sequences of the following receptors were a kind gift from Dr. Bryan Roth

98   (University of North Carolina, NC; Addgene kit no. 1000000068) [31] and were used for subcloning

99   into pcDNA3.1 plasmids removing V2-tail, TEV site, and tTA sequences: follicle-stimulating

100 hormone receptor (FSHR), cannabinoid receptor 1 (CB1R), cannabinoid receptor 2 (CB2R),

101 sphingosine-1 phosphate receptor 1 (S1PR1), lysophosphatidic acid 2 receptor (LPAR2),

102 somatostatin receptor 1 (SSTR1), neuropeptide FF receptor 1 (NPFFR1), free fatty acid receptor

103 3 (FFA3R), galanin 1 receptor (GALR1), formyl peptide receptor 1 (FPR1), hydroxycarboxylic acid

104 receptor 2 (HCAR2), neuropeptide Y receptor Y1 (NPYR1), protease-activated receptor 1 (PAR1),

105 protease-activated receptor 2 (PAR2), histamine receptor H3 (HRH3), dopamine D1 receptor

4

106   (D1R), dopamine D3 receptor (D3R), adenosine A2B receptor (ADORA2B), parathyroid hormone

107   1 receptor (PTH1R), melanocortin 4 receptor (MC4R), and calcitonin-like receptor (CLR).

108   Plasmids encoding the cAMP sensor (pGloSensor™-22F) and CRE-Nluc reporter were

109   purchased from Promega. pFL-tk encoding firefly luciferase under the control of constitutively

110   active thymidine kinase promoter was used as a normalizer for reporter assays. The plasmids

111   encoding the following G_s-derived chimeras were a kind gift from Dr. Robert Lucas (University of

112   Manchester, UK)[27]: GsGz (Addgene plasmid #109355), GsGo (Cys) (Addgene plasmid #109375),

113   GsGi (Cys) (Addgene plasmid #109373). pOZITX-S1 was a kind gift from Jonathan Javitch

114   (Addgene plasmid #184925). All constructs were verified by Sanger sequencing.

115   A modular plasmid system was used to assemble the components of G_ZESTY into single

116   multicomponent plasmids. Five insert shuttle plasmids (P1-P5) and a destination plasmid were

117   constructed with matching homology regions for Gibson assembly flanking an insert sequence.

118   For assembly, the shuttle plasmids and destination plasmid were digested with the Type IIS

119   restriction enzyme CspCI, which possesses a relatively rare 7-bp recognition sequence. As CspCI

120   is a type IIS restriction sequence, it cleaves outside of its recognition sequence, allowing for

121   generation of DNA fragments containing unique ends for homology-directed assembly (i.e.

122   Gibson assembly). P1 contained a short CMV promoter (lacks CspCI site found in conventional

123   CMV promoter) driving expression of GloSensor-22F, P2 contained a short ubiquitin C promoter

124   (UbC) driving expression of PTX-S1, P3 contained an ampicillin selection marker and a short

125   CMV promoter driving expression of the receptor of interest, P4 was generally a blank insert

126   except for the GABAB receptor for which P4 contained a short CMV promoter driving expression

127   of the GABAB receptor subunit 2 (with P3 containing subunit 1), and P5 contained a UbC promoter

128   driving expression of the GsGz chimera. To generate plasmids only containing some of these

129   inserts of interest, blank inserts were used for any of P1-P5 containing G_ZESTY components not

130   required. The destination plasmid was a pUC57-Kan containing the homologous sequences for

131   Gibson assembly of the inserts. Of note, a plasmid with an alternate resistance marker to AmpR

132   was used as this allows for selection of the final assembled clone without any carry-through of

133   undigested insert plasmids. The CspCI digest contained 110 fmol of each insert plasmid (~375

134   ng for a 5 kb insert plasmid), 37.5 fmol of the destination plasmid (~125 ng for a 5 kb destination

135   plasmid), 5 µL rCutSmart buffer (NEB), and 1 µL CspCI (5,000 units/mL; NEB) in a 50 µL reaction,

136   incubated at 37 °C for 1 hour, and heat inactivated at 65 °C for 20 minutes. For the Gibson

137   assembly, 5 µL of the CspCI digest was mixed with 5 µL of NEBuilder HiFi DNA Assembly Master

138   Mix (NEB), incubated at 50 °C for 15 minutes. For transformation of the assembled plasmid, 1.5

139   µL of the Gibson assembly mix was transformed into either NEB 5-alpha Competent *E. coli* (NEB)

5

140   or NEB 10-beta Electrocompetent *E. coli* (NEB) and plate on selective LB agar containing both

141   kanamycin (selects for destination plasmid backbone) and ampicillin (selects for P3 insert).

142

2.3 Chemicals

144   The following chemicals were purchased: clonidine (Tocris), dopamine (Tocris), GABA (Tocris),

145   serotonin (Tocris), 1-oleoyl lysophosphatidic acid (Tocris), DAMGO (MedChemExpress), TFLLR

146   (MedChemExpress), human PAR-2 (1-6, SLIGKV) (MedChemExpress), human galanin (1-30)

147   (MedChemExpress), IBMX (MedChemExpress), SEW2871 (MedChemExpress), somatostatin-

148   14 (Cpc Scientific), human neuropeptide Y (13-36) (Cpc Scientific), neuropeptide FF (Thermo

149   Scientific Chemicals), MK-6892 (MedChemExpress), 2-arachidonoyl glycerol (Cayman

150   Chemicals), N-Formyl-Met-Leu-Phe (R&D systems), SNC80 (Adipogen), isobutyric acid (TCI

151   chemicals), salvinorin A (ChromaDex Inc.), morphine (Mallinckrodt Chemical Company), human

152   β-endorphin (Sigma-Aldrich), teriparatide (MedChemExpress), NDP-α-MSH (Phoenix

153   Pharmaceuticals), AB-MECA (MedChemExpress), quinpirole (Tocris), calcitonin gene-related

154   peptide (CGRP) (AnaSpec).

2.5 cAMP measurements using G$_Z$ESTY

156   HEK293T/17 cells were transfected as described above with pGloSensor™-22F cAMP plasmid

157   (Promega) and indicated plasmids for mammalian expression of GPCRs, PTX-S1 (or OZITX-S1),

158   and Gs-based chimeras (GsGo, GsGi, or GsGz). 18 hours post-transfection, cells were

159   mechanically detached using a gentle stream of PBS, centrifuged at 500 g for 5 minutes, and

160   resuspended in 300 µl of PBS containing 0.5 mM MgCl$_2$ and 0.1% glucose. 40 µl of the cell

161   suspension were transferred to each well of 96-well flat-bottomed white plates (Greiner Bio-One).

162   D-Luciferin potassium salt (Gold Bio; #DLUCK100) was dissolved in HEPES buffer 10 mM pH 7.4

163   to obtain a 5x stock at 30 mg/mL. 10 µL of 5X D-luciferin solution were added to the cells. Cells

164   were then incubated at 37°C and 5% CO$_2$ for 1 hour and then equilibrated in the plate reader at

165   28°C, until stable baseline values were reached (~15 minutes). The luminescence signal was

166   monitored approximately every 30 seconds using a POLARstar Omega microplate reader (BMG

167   Labtech).

168   In assays performed on coated 96 well plates, cells were transfected in 6-well plates. The day

169   after transfection, the media was removed, and cells were gently washed with PBS once and

170   briefly trypsinized with 100 µL of trypsin. Trypsinization was blocked by the addition of 900 µL of

171   transfection media containing 10% FBS, cells were counted and seeded at 6.5 × 10^4 cells/well on

172   a sterile white 96-well plate coated with poly-D-lysine. Cells were then incubated overnight at

173   37°C and 5% CO_2. 24 hours later, media in each well was replaced with 40 µL of PBS containing

174   0.5 mM $MgCl_2$, 0.1% glucose, and 10 µL of 5X D-Luciferin, and then incubated for 1h at 37°C.

175   The 96-well plate was moved into the plate reader, equilibrated at 28°C until stable luminescence

176   values were obtained and finally treated according to the experiment setup.

2.6 G protein nanoBRET assay

178   GPCR activation in live cells was measured as BRET signal between Venus-Gβ1γ2 and

179   masGRK3CT-Nluc performed as described previously[23]. 2.5 µg of total DNA was transfected

180   according to the following ratio: 0.21 µg of Gβ1-Venus(156-239); 0.21 µg of Gγ2-Venus(1-155);

181   0.21 µg of masGRK3CT-Nluc; 0.42 µg of $G\alpha_{oA}$ proteins; and 0.21 µg of receptor. Empty vector

182   pcDNA3.1 was used to normalize the amount of transfected DNA. 18 hours after transfection,

183   HEK293T/17 cells were washed once with PBS. Cells were then mechanically harvested using a

184   gentle stream of PBS, centrifuged at 500 g for 5 minutes, and resuspended in 500 µl of PBS

185   containing 0.5 mM $MgCl_2$ and 0.1% glucose. 25 µl of resuspend cells were distributed in 96-well

186   flat-bottomed white microplates (Greiner Bio-One). The Nluc substrate, furimazine (N1120;

187   Promega) was used according to the manufacturer's instructions. Luminescence was quantified

188   at room temperature using a POLARstar Omega microplate reader (BMG Labtech). BRET signal

189   was determined by calculating the ratio of the light emitted by Venus-Gβ1γ2 (collected using the

190   emission filter 535/30) to the light emitted by masGRK3CT-Nluc (475/30). The average baseline

191   value (basal BRET ratio) was recorded for 5 seconds before agonist application.

2.7 CRE luciferase reporter assay

193   HEK293T/17 cells were plated at a density of 1×10^6 cells/well in 6-well plates in an antibiotic-

194   free medium and transfected as described above. 2.5 µg of total DNA was transfected according

195   to the following ratio: 0.10 µg of pFL-tk plasmid expressing firefly luciferase under control of the

196   constitutive thymidine kinase promoter; 0.21 µg of CRE-Nluc luciferase reporter; 1.98 µg of

197   GPCR; and only in experiments screening $G_{i/o}$ activation, 0.21 µg of GsGi1 chimera. pcDNA3.1

198   was used to normalize the amount of transfected DNA. Cells were incubated overnight and then

199   serum-starved in Opti-MEM for 4 hours before collection. Transfected cells were harvested using

200   a gentle stream of PBS, centrifuged for 5 minutes at 500 ×g, and resuspended in 150 µl of PBS

201   containing 0.5 mM $MgCl_2$ and 0.1% glucose. 30 µl of cells were incubated in 96-well flat-bottomed

202   white microplates (Greiner Bio-One) with 30 µl of luciferase substrate according to manufacturers'

203   instructions: furimazine (Promega NanoGlo; N1120) for Nluc, and D-luciferin (Promega BrightGlo;

204   E2610) for firefly luciferase. Luciferase levels were quantified using a POLARstar Omega

205   microplate reader (BMG Labtech). Firefly luciferase expression was used to normalize the signal

206   and compensate for variability due to transfection efficiency and number of cells.

207   **2.8 Mice**

208   C57BL/6J mice were housed in a temperature and humidity-controlled room in the vivarium of the

209   University of Rochester on a 12:12-h light/dark cycle (lights off at 18:00 h) provided with food and

210   water ad libitum. Male and female adult mice were used for the experiments. Mice were sacrificed

211   by cervical dislocation, the head was removed and placed immediately in a microwave at

212   maximum power for 10s to block protease activity[36]. One brain was removed and immediately

213   homogenized in a glass-glass homogenizer with 4mL of PBS. Homogenate was then sonicated

214   three times on ice for 10s at 30% power and spun for 10 min at 14,000g at 4°C. 50 μL of

215   supernatant was then applied to the cells. All procedures were pre-approved and carried out

216   following the University Committee on Animal Resources (UCAR) at the University of Rochester.

217   Bovine pituitary extract was purchased from MP biologicals (cat#2850450).

218   **2.9 Statistical analysis**

219   Statistical analysis was performed using GraphPad Prism 9 software. The number of replicates

220   and type of statistical analysis used are described in each figure legend.

221

222   **3. RESULTS**

223   **3.1 G_s-based protein chimeras combined with a cAMP biosensor allow for the**

224   **measurement of the activation of $G_{i/o/z}$-coupled receptors.**

225   Several cell-based assays are currently available to study the activation of $G_{i/o/z}$-coupled

226   receptors. In the G protein nanoBRET assay, receptor activation in response to ligands is

227   measured as an increase in BRET signal due to the release of Gβγ-venus and its interaction with

228   a membrane-anchored biosensor that consists of the C-terminus of GRK3 fused to Nluc

229   (**Supplementary Figure 1A**)[22,35]. The main advantage of this assay is the rapid measurement of

230   a proximal event in GPCR activation that allows for real-time analysis of the receptor kinetics but

231   with a trade-off in assay sensitivity (**Supplementary Figure 1D**). Genetic reporters expressing

232   luciferase under the control of a GPCR-inducible promoter are commonly used. These assays

233   have been developed to detect signals downstream of GPCR coupling to G_s (CRE-luc reporter),

234   G_q (NFAT-luc reporter), and $G_{12/13}$ (SRE-luc reporter)[32]. Activation of $G_{i/o/z}$-coupled receptors can

235   be quantified as a reduction in the luciferase accumulation using a CRE-luc reporter, or indirectly

236   as Gβγ modulation of signaling pathways regulating the SRE-luc reporter. A more sensitive

8

237 approach adopts G protein chimeras based on the core of $G\alpha_s$ or $G\alpha_q$ and the last few amino

238 acids of members of the $G_{i/o/z}$ family[37,38]. This strategy allows the detection of an accumulation of

239 luciferase using CRE-luc and NFAT-luc, respectively, in response to the activation of $G_{i/o/z}$-

240 coupled receptors (**Supplementary Figure 1B**). One limitation of this approach is that the

241 receptor must be exposed to an agonist for an extended time to accumulate measurable

242 quantities of luciferase in the cell (**Supplementary Figure 1D**). During this time, processes like

243 receptor desensitization, internalization, and compensatory mechanisms can take place in the

244 cell reducing the assay reliability. A good compromise between speed and assay sensitivity is

245 based on measuring the accumulation of second messengers. Activation of $G_{i/o/z}$-coupled

246 receptors inhibits the activity of adenylyl cyclase thereby reducing cAMP accumulation in

247 response to forskolin treatments. Real-time measurements of cAMP levels can rapidly indicate if

248 a $G_{i/o/z}$-coupled receptor has been activated. This assay depends on the side-by-side comparison

249 of cAMP accumulation in cells treated with an agonist and in cells treated with vehicle. Such an

250 approach is rapid, achieving a signal plateau within 15 minutes of agonist application

251 (**Supplementary Figure 1C-D**). Alternatively, co-expression of $G\alpha_s$-based chimeras bearing the

252 C-terminus of $G_{i/o/z}$ family members can be used to redirect receptor activation to stimulate

253 adenylyl cyclase and cAMP accumulation (**Supplementary Figure 1C-D**)[27]. Overall, this last

254 strategy yields an optimal balance between assay duration and sensitivity.

255 Building on these observations, we tested the activation of four prototypical $G_{i/o/z}$-coupled

256 GPCRs, dopamine D2 receptor (D2R), α2 adrenergic receptor (ADRA2A), γ-aminobutyric acid B

257 receptor (GABAB), and μ opioid receptor (MOR) using three $G\alpha_s$-based chimeras bearing the C-

258 terminus of $G\alpha_i$, $G\alpha_o$, and $G\alpha_z$. Application of selective agonists revealed a robust accumulation

259 of intracellular cAMP as measured using a split-luciferase GloSensor (**Figure 1A**). We measured

260 baseline luminescence for 3 minutes before applying each agonist as well as the maximal

261 amplitude obtained in response to agonist stimulation (**Figure 1B**). Using these measurements,

262 we calculated the fold change induction for each condition as an index that we can use to compare

263 sensitivity between assays (**Figure 1C**). These experiments revealed that the GsGz chimera

264 always showed a low baseline that contributed to the highest fold change observed with three out

265 of four receptors.

266

267 **3.2 The assay sensitivity shows a clear dependence on both the transfection ratio of assay**

268 **components and the inhibition of endogenous $G_{i/o}$ proteins.**

269 We optimized the assay conditions by adjusting the amount of transfected plasmids used

270 to express each $G\alpha_s$-chimera. (**Figure 2A**). We found that, generally, excessive amounts of $G\alpha_s$-

271   chimeras result in higher baselines, which attenuate the observed fold change (**Supplementary**

272   **Figure 2**). Moreover, considering that GsGz, just like $G\alpha_z$, is insensitive to the action of pertussis

273   toxin (PTX), we introduced it in the assay aiming to reduce the adenylyl cyclase inhibition due to

274   endogenous $G\alpha_{i/o}$ proteins. We found that very low levels of transfected PTX boosted the

275   induction of cAMP for each GPCR from a minimum of 1.5 times (GABABR) to a maximum of 6.1

276   times (D2R) (**Figure 2B; Supplementary Figure 3**). Similarly, keeping a fixed amount of PTX,

277   we titrated the amount of the GsGz chimera. We observed comparable effects with each of the

278   four receptors indicating an optimal amount of GsGz at 45-138 ng over a total of 2.5 µg of

279   transfected DNA (**Figure 2C; Supplementary Figure 4**). Finally, we observed that the greatest

280   accumulation of cAMP was achieved when transfecting the highest amount of receptor (**Figure**

281   **2D; Supplementary Figure 5**). Based on these results, we recalibrated the amount of each

282   transfected plasmid, expressing the four assay components, and determined the optimal

283   conditions as a molar ratio of 50:47.5:1.8:0.7 (GloSensor:GPCR:GsGz:PTX) (**Figure 2E**). These

284   optimization steps led to an overall 3-6 fold improvement in assay sensitivity measured as a fold

285   change accumulation in cAMP. Given that HEK293 cells express $G\alpha_z$[39], we explored if

286   transfecting cells with the catalytic subunit of OZITX instead of PTX would further boost the signal

287   because it inhibits each $G_{i/o/z}$ protein including G_z[40]. We initially verified the effect of OZITX on the

288   activation of wild-type $G_{i/o/z}$ proteins and G protein chimeras using the G protein nanoBRET assay

289   (**Supplementary Figure 6A**). Our data indicate a complete abolishment of signal initiated by wild

290   type $G\alpha_o$, $G\alpha_i$, and $G\alpha_z$, while the inhibition of the Gs-based chimeras was minimal for GsGo and

291   GsGz, and more pronounced but incomplete for GsGi (**Supplementary Figure 6B**). We then

292   incorporated OZITX in our assay and tested the activation of D2R, GABABR, ADRA2A, and MOR.

293   Our findings indicate that, overall, OZITX demonstrated a comparable effect to PTX, with no

294   significant enhancement observed in the assay. (**Supplementary Figure 6C**).

295

296   **3.3 Multiple conditions can further affect signal detection in G_zESTY.**

297   Further conditions can significantly affect assay sensitivity. As previously reported[28], we

298   first confirmed that GloSensor assays produce a greater signal when performed at 28°C

299   compared to 23°C or 37°C (**Figure 3A; Supplementary Figure 7**). Moreover, the presence of

300   ligands in the culturing media can affect GPCR activation because of desensitization processes.

301   We tested this factor by serum starving the cells for 4 hours or changing the cell culture media

302   after transfection to one containing 10% charcoal-stripped FBS or 10% dialyzed FBS (**Figure 3B;**

303   **Supplementary Figure 8**). Our data showed that these four prototypical GPCRs are generally

304   not affected by the presence of normal serum, or they are negatively impacted by its absence.

305   Furthermore, many GPCRs have been shown to interact with extracellular matrix components[41] and, therefore, the analysis of their signaling properties may be different if studied using cells in adhesion or in suspension. We tested the same four GPCRs in these two conditions and we found that, indeed, GABAB receptor shows a significantly higher signal when cells are cultured in poly-D-lysine coated wells (**Figure 3C; Supplementary Figure 9**). Finally, we tested the possible advantage of blocking endogenous phosphodiesterases (PDEs) with IBMX to enhance the accumulation of cAMP (**Figure 3D; Supplementary Figure 10)**. As expected, we found that applying IBMX before recording the baseline significantly increased the baseline reading and reduced the overall fold change observed. However, when IBMX was applied at the same time as the agonist, we measured a significant increase in signal (**Figure 3D; Supplementary Figure 10**). By subtracting the signal obtained by applying IBMX with the vehicle from the total luminesce observed, we found that the increased signal was not simply due to the simultaneous activation of adenylyl cyclase and inhibition of PDEs.

318   To quantify the robustness of G_zESTY, we calculated a screening window coefficient (Z factor). This factor reflects both the dynamic range of the assay and its variability, and it is a significant metric of the assay quality. Considering the overall goal of using G_zESTY for GPCR deorphanization where agonists are normally not available, we calculated the Z factor in two different conditions. We first compared cells transfected with D2R or GABAB receptors and treated with the respective agonist vs vehicle (**Figure 3E; Supplementary Figure 11A**). Then, we analyzed the effect of agonist treatments on cells expressing each GPCR vs mock-transfected cells (**Figure 3F; Supplementary Figure 11B**). This condition mimics the conditions for high-throughput screening to identify orphan GPCR ligands. Independent replicates conducted on different days demonstrated that the assay is highly reproducible, with Z factors calculated at 0.75 and 0.83 for D2R, and 0.78 for both conditions for the GABAB receptor (**Figure 3G; Supplementary Figure 11C**).

330

331   **3.4 Generation of an all-in-one plasmid for G_zESTY cell delivery.**

332   Like most cell-based systems used to detect GPCR signaling, G_zESTY is a multicomponent assay (**Figure 4A**). As a result, functional measurements require efficient co-delivery of multiple plasmids in each cell. This issue is normally overcome by averaging the signal of a large number of cells assuming that a significant fraction will express all the components. We recently generated a facile system to produce large plasmids encoding multiple proteins under the control of individual promoters. This approach guarantees that each transfected cell will express all of the necessary components, thereby increasing the assay's sensitivity and

339   simplifying transfection protocols. To select promoters to drive the expression of each component

340   recapitulating our previously defined ratios, we performed a promoter efficiency assay (**Figure**

341   **4B**). Based on these results, we selected a minimal CMV promoter to express the GloSensor and

342   GPCRs, and a UbC promoter for the expression of PTX-S1 and GsGz. We subcloned each

343   component accordingly and generated a set of all-in-one plasmids (**Figure 4C**). We then tested

344   these newly generated tools in cells transiently transfected with each of our four prototypical $G_{i/o/z}$-

345   coupled receptors that we stimulated with selective agonists. We found that the 4-in-one plasmids

346   performance was comparable to the co-transfection of multiple plasmids, but greatly simplified

347   transfection protocols and reproducibility (**Figure 4D**).

348   Next, we expanded the analysis of G_zESTY capabilities to a larger array of 24 $G_{i/o/z}$-

349   coupled GPCRs paired with the 3-in-one construct. We confirmed the suitability of the assay to

350   study the pharmacology of 23 out of 24 $G_{i/o/z}$-coupled receptors (**Figure 5A** and **5C**). At the same

351   time, we confirmed that in our setup we can still detect the activation of 5 G_s-coupled receptors

352   (**Figure 5A**). Overall, this data demonstrated that G_zESTY is a powerful tool for GPCR

353   deorphanization as it sensitively detects activation of both $G_{i/o/z}$- and G_s-coupled GPCRs,

354   potentially enabling the study of 86% of the GPCRome and, by similarity, most of the orphan

355   GPCRs (**Figure 5B**). We next investigated if G_zESTY was suitable to detect partial agonism.

356   Using MOR as a model, we obtained concentration-response curves after stimulation with the

357   endogenous ligand β-endorphin (pEC50=5.45, E_{max}=62.91), with the full agonist DAMGO

358   (pEC50=7.17; E_{max}=59.53), and with the partial agonist morphine (pEC50=7.21, E_{max}=38.85) that

359   showed 65% of the maximal amplitude measured with DAMGO (**Figure 6A**). We also

360   demonstrated that G_zESTY can be used to study the activation of endogenously expressed

361   receptors. To this goal, concentration-response curves were obtained from cells transfected with

362   the 3-in-one construct, which does not express any exogenous GPCR, and treated with selective

363   peptidic agonists activating endogenously expressed protease-activated receptor (PAR) PAR1

364   (pEC50=4.56, E_{max}=73.87) or PAR2 (pEC50=4.97, E_{max}=103.70). Cells transfected with the 2-in-

365   one construct (no GsGz chimera) served as negative control (**Figure 6B**).

366

367   **3.5 G_zESTY application to GPCR deorphanization.**

368   To assess the suitability of G_zESTY in projects aiming at the identification of endogenous

369   ligands for orphan GPCRs, we treated cells co-transfected with the 3-in-one plasmid and

370   individual GPCRs with a raw source of endogenous ligands. Historically, similar strategies were

371   successfully used to isolate anandamide from pig brain, identifying it as an endogenous ligand for

372   cannabinoid receptors[42]; these methods also facilitated the identification of ghrelin from rat

373   stomach extract[43], and helped pair other GPCRs with their endogenous ligands[44-47]. To this goal,

374   we prepared a crude aqueous mouse brain extract that we applied to G_zESTY-transfected cells,

375   and we measured cAMP accumulation over time (**Figure 6C**). Control cells transfected with the

376   3-in-one plasmid and therefore expressing GloSensor, GsGz, and PTX, but not exogenous

377   GPCRs, showed significant induction of cAMP levels likely due to the activation of endogenous

378   receptors. This baseline was used to normalize the signal obtained from cells overexpressing

379   exogenous GPCRs. Applying this strategy, we demonstrated that the high sensitivity of G_zESTY

380   enables the detection of robust and consistent activation of D2R, ADRA2A, GABAB, and MOR

381   from crude brain extracts, which likely contain highly diluted endogenous agonists (**Figure 6D**).

382   We next apply the same strategy to explore the possible activation of a battery of orphan GPCRs

383   from crude brain extracts. Intriguingly, we detected a consistent activation of orphan receptors

384   GPR176 and GPR37 suggesting a significant presence of their endogenous ligands in the mouse

385   brain (**Figure 6E**). Both these orphan GPCRs are expressed in the brain, and they are reported

386   to couple to heterotrimeric G proteins of the $G_{i/o/z}$ family, but their endogenous ligands have not

387   been identified or agreed upon[48-50]. We performed parallel experiments using the same strategy

388   to test the presence of GPCR ligands in bovine pituitary extracts. We reasoned that many GPCRs

389   are activated by hormones released by glands, and we used the follicle-stimulating hormone

390   (FSH) receptor as a positive control, as its endogenous ligand is secreted by the pituitary gland.

391   We found that pituitary extract can indeed activate FSHR, and we measured some level of

392   activation of GABAB receptor, but none of the orphan GPCRs we tested were activated

393   (**Supplementary Figure 12**).

394

395   **4. DISCUSSION**

396   Orphan GPCRs, by definition, have unknown or poorly understood ligands and signaling

397   mechanisms. Without a known ligand or baseline receptor activity, designing assays to measure

398   their activation or inhibition becomes a complex task. A major obstacle in identifying endogenous

399   ligands for orphan GPCRs is the absence of sensitive assays capable of detecting low

400   concentrations of these ligands in biological samples. This challenge is especially pronounced for

401   orphan GPCRs that couple to heterotrimeric G proteins of the $G_{i/o/z}$ family, which, according to the

402   G protein database (GPCRdb.org), represent 72% of deorphanized GPCRs, with 30% being

403   uniquely coupled to $G_{i/o/z}$ proteins[51,52]. To address this problem, we designed G_zESTY, an

404   optimized cell-based assay that enables robust detection of GPCR activation in response to both

405   purified ligands and mixed sources of molecules, including those containing diluted ligands.

406   Our work identified optimal assay conditions that apply to each GPCR tested, such as the
407   temperature of the assay, ratio of assay components, and presence of IBMX, while other
408   parameters appear to affect the readout in a GPCR-specific manner. For example, we did not
409   observe a significant effect of serum on the assay outcome for four prototypical GPCRs tested,
410   however, the presence of ligands in the culture media has been shown to induce receptor
411   desensitization and internalization halting the access of extracellular ligands to the receptor
412   itself[53-55]. Therefore, we cannot exclude the possibility that testing certain GPCRs may benefit
413   from using reduced serum content or dialyzed serum. This aspect will require specific assessment
414   for individual receptors. Using IBMX has the advantage of enhancing the detected signal, thereby
415   improving the assay's sensitivity. Additionally, it helps eliminate false positives in high-throughput
416   screens caused by the presence of phosphodiesterase inhibitors in many compound libraries. By
417   applying innovative cloning techniques, we generated large plasmids that encode multiple
418   proteins under the control of unique promoters. These all-in-one plasmids have the advantage of
419   expressing each component at precisely defined and optimized ratios. Moreover, their use greatly
420   simplifies transfection protocols for large-scale screening efforts. Using all-in-one plasmids, we
421   showed that G_zESTY is suitable to detect the activation of endogenously expressed receptors.
422   Delivery of the 3-in-one plasmid to relevant cell types can be combined with agonist treatment to
423   perform pharmacological studies of receptors of interest in a physiologically relevant context. Our
424   initial optimization steps for G_zESTY were performed using four prototypical GPCRs (D2R,
425   ADRA2A, GABAB, and MOR). The optimized protocol was later applied to an array of 24 $G_{i/o/z}$-
426   coupled GPCRs. The results showed that the great majority exhibited over a 20-fold change in
427   signal compared to baseline, suggesting ideal signal-to-noise properties for the assay. We also
428   observed smaller signal amplitude for a few receptors. This lower sensitivity may depend on
429   several factors including the presence of endogenous agonists in the culture media that can lead
430   to receptor desensitization or the requirement of performing the assay with cells in adhesion.
431   Transfected receptors may also not be properly expressed, targeted to the plasma membrane, or
432   require accessory proteins to generate functional receptor complexes. Therefore, when working
433   with a specific receptor it is recommended to test multiple assay conditions in the cell type of
434   choice to achieve an optimal assay sensitivity.

435   Screening efforts to identify orphan GPCR agonists will be markedly enhanced by utilizing
436   G_zESTY. Analysis of the constitutive activity of orphan GPCRs provides valuable information
437   regarding their G protein coupling profile[35,56,57]. Recent studies have shown that, similar to ligand-
438   activated GPCRs, the majority of orphan GPCRs couple to heterotrimeric G proteins of the $G_{i/o/z}$
439   family. This makes them suitable candidates for analysis using G_zESTY. Furthermore, given the

440   limited understanding of the G protein coupling profile for many orphan GPCRs, a key benefit of

441   G_zESTY is its ability to detect the activation of approximately 86% of GPCRs. This estimate is

442   based on coupling data regarding the number of GPCRs that can couple to G_s and/or $G_{i/o/z}$

443   proteins (**Figure 5B**).

444   The isolation of orphan GPCR endogenous ligands relies significantly on the availability

445   of methods that can accurately detect their presence in raw unfractionated extracts. In this study,

446   we utilized G_zESTY to identify the existence of endogenous ligands for orphan GPCRs in the

447   mouse brain. Our approach consistently detected known neurotransmitters capable of activating

448   adrenergic, dopaminergic, GABAergic, and opioid receptors, thereby validating the method.

449   Notably, we also identified the presence of ligands that can activate class A orphan receptors

450   GPR176 and GPR37. GPR176 was previously found to be enriched in the mouse

451   suprachiasmatic nucleus (SCN) of the hypothalamus, the central pacemaker that controls the

452   circadian rhythm[48,58]. Its protein expression levels oscillate according to the circadian period being

453   higher during the night, and GPR176-deficient mice display a significantly shorter circadian period

454   compared to their wild-type littermates. Further studies indicated that GPR176 is probably not a

455   light signal-related receptor for the SCN; rather, it seems to be involved in determining the intrinsic

456   period of the SCN. Finally, heterologous expression of GPR176 blunted the forskolin-induced

457   accumulation of cAMP suggesting its coupling to heterotrimeric $G_{i/o/z}$ proteins[48]. Overall, these

458   findings indicate that GPR176 is involved in the suppression of cAMP production in the SCN

459   during nighttime, which serves as the molecular mechanism for its regulation of the circadian

460   period[59]. GPR176 roles outside the central nervous system have also been described[60]; however,

461   no endogenous or synthetic ligands capable of activating GPR176 have been identified yet. With

462   G_zESTY enabling the detection of GPR176 endogenous ligand in the mouse brain, we will be

463   able to perform further studies leading to its isolation. GPR37 is a brain-enriched orphan GPCR

464   with some of the highest transcript levels among all GPCRs[61]. Despite its well-studied involvement

465   in Parkinson's disease, inflammatory responses, and pain, the identity of its endogenous ligand

466   remains a topic of debate[49,62-64]. Early studies proposed prosaptide, a fragment of the secreted

467   neuroprotective and glioprotective factor prosaposin, as the endogenous ligand for GPR37[50]. The

468   identity of this ligand-receptor pair was supported by the fact that prosaptide stimulation of cells

469   transfected with GPR37 induced ERK phosphorylation in a PTX-sensitive manner suggesting

470   coupling to $G_{i/o}$ proteins[50]. Moreover, ^{35}S-GTPγS binding assays and inhibition of forskolin-

471   induced cAMP accumulation all pointed at prosaptide as the endogenous ligand for GPR37[50].

472   GPR37 activation by prosaptide was later confirmed by measuring a PTX-sensitive intracellular

473   calcium mobilization in GPR37 transfected HEK293 cells[65]. In the same study, activation by

15

474   neuroprotectin D1 was also observed. Studies in astrocytes also detected GPR37 activation by

475   prosaptide[66]. However, the claim that prosaposin and prosaptide are the endogenous ligands for

476   GPR37 was later challenged by reports demonstrating that GPR37 shows high constitutive

477   activity and that prosaptide treatments were ineffective (Smith, 2015). Consequently, the

478   prosaptide/GPR37 pairing has yet to be approved by the International Union of Basic and Clinical

479   Pharmacology (IUPHAR) Nomenclature Committee. Given that multiple endogenous ligands can

480   activate the same receptor[8], the pursuit of identifying GPR37 ligands detected using G_ZESTY is

481   a valuable endeavor.

482

483   **Acknowledgments:**

References

1. Insel, P. A. *et al.* GPCRomics: An Approach to Discover GPCR Drug Targets. *Trends in pharmacological sciences* **40**, 378-387, doi:10.1016/j.tips.2019.04.001 (2019).

2. Sriram, K. & Insel, P. A. G Protein-Coupled Receptors as Targets for Approved Drugs: How Many Targets and How Many Drugs? *Molecular pharmacology* **93**, 251-258, doi:10.1124/mol.117.111062 (2018).

3. Gomes, I. *et al.* GPR171 is a hypothalamic G protein-coupled receptor for BigLEN, a neuropeptide involved in feeding. *Proc Natl Acad Sci U S A* **110**, 16211-16216, doi:10.1073/pnas.1312938110 (2013).

4. Gomes, I. *et al.* Identification of GPR83 as the receptor for the neuroendocrine peptide PEN. *Sci Signal* **9**, ra43, doi:10.1126/scisignal.aad0694 (2016).

5. Yosten, G. L. *et al.* GPR160 de-orphanization reveals critical roles in neuropathic pain in rodents. *J Clin Invest* **130**, 2587-2592, doi:10.1172/JCI133270 (2020).

6. Franchini, L. & Orlandi, C. Probing the orphan receptors: Tools and directions. *Prog Mol Biol Transl Sci* **195**, 47-76, doi:10.1016/bs.pmbts.2022.06.011 (2023).

7. De Giovanni, M. *et al.* GPR35 promotes neutrophil recruitment in response to serotonin metabolite 5-HIAA. *Cell* **185**, 815-830 e819, doi:10.1016/j.cell.2022.01.010 (2022).

8. Foster, S. R. *et al.* Discovery of Human Signaling Systems: Pairing Peptides to G Protein-Coupled Receptors. *Cell* **179**, 895-908 e821, doi:10.1016/j.cell.2019.10.010 (2019).

9. Liberles, S. D. & Buck, L. B. A second class of chemosensory receptors in the olfactory epithelium. *Nature* **442**, 645-650, doi:10.1038/nature05066 (2006).

10. Isberg, V. *et al.* Computer-aided discovery of aromatic l-alpha-amino acids as agonists of the orphan G protein-coupled receptor GPR139. *J Chem Inf Model* **54**, 1553-1557, doi:10.1021/ci500197a (2014).

11. Southern, C. *et al.* Screening beta-arrestin recruitment for the identification of natural ligands for orphan G-protein-coupled receptors. *J Biomol Screen* **18**, 599-609, doi:10.1177/1087057113475480 (2013).

12. Graaf, C. *et al.* Glucagon-Like Peptide-1 and Its Class B G Protein-Coupled Receptors: A Long March to Therapeutic Successes. *Pharmacological reviews* **68**, 954-1013, doi:10.1124/pr.115.011395 (2016).

13. Goke, R. & Conlon, J. M. Receptors for glucagon-like peptide-1(7-36) amide on rat insulinoma-derived cells. *J Endocrinol* **116**, 357-362, doi:10.1677/joe.0.1160357 (1988).

14. Shimizu, I., Hirota, M., Ohboshi, C. & Shima, K. Identification and localization of glucagon-like peptide-1 and its receptor in rat brain. *Endocrinology* **121**, 1076-1082, doi:10.1210/endo-121-3-1076 (1987).

15. Thorens, B. Expression cloning of the pancreatic beta cell receptor for the gluco-incretin hormone glucagon-like peptide 1. *Proceedings of the National Academy of Sciences of the United States of America* **89**, 8641-8645, doi:10.1073/pnas.89.18.8641 (1992).

16. Graziano, M. P., Hey, P. J., Borkowski, D., Chicchi, G. G. & Strader, C. D. Cloning and functional expression of a human glucagon-like peptide-1 receptor. *Biochemical and biophysical research communications* **196**, 141-146, doi:10.1006/bbrc.1993.2226 (1993).

17. Dillon, J. S. *et al.* Cloning and functional expression of the human glucagon-like peptide-1 (GLP-1) receptor. *Endocrinology* **133**, 1907-1910, doi:10.1210/endo.133.4.8404634 (1993).

18. Knudsen, L. B. & Lau, J. The Discovery and Development of Liraglutide and Semaglutide. *Front Endocrinol (Lausanne)* **10**, 155, doi:10.3389/fendo.2019.00155 (2019).

19. ElSayed, N. A. *et al.* 9. Pharmacologic Approaches to Glycemic Treatment: Standards of Care in Diabetes-2023. *Diabetes Care* **46**, S140-S157, doi:10.2337/dc23-S009 (2023).

20. FDA. FDA Approves New Drug Treatment for Chronic Weight Management, First Since 2014. (2021).

543 21 Olsen, R. H. J. *et al.* TRUPATH, an open-source biosensor platform for interrogating the
544   GPCR transducerome. *Nature chemical biology* **16**, 841-849, doi:10.1038/s41589-020-
545   0535-8 (2020).
546 22 Hollins, B., Kuravi, S., Digby, G. J. & Lambert, N. A. The c-terminus of GRK3 indicates
547   rapid dissociation of G protein heterotrimers. *Cellular signalling* **21**, 1015-1021,
548   doi:10.1016/j.cellsig.2009.02.017 (2009).
549 23 Masuho, I. *et al.* Distinct profiles of functional discrimination among G proteins determine
550   the actions of G protein-coupled receptors. *Science signaling* **8**, ra123,
551   doi:10.1126/scisignal.aab4068 (2015).
552 24 Jang, W., Lu, S., Xu, X., Wu, G. & Lambert, N. A. The role of G protein conformation in
553   receptor-G protein selectivity. *Nat Chem Biol*, doi:10.1038/s41589-022-01231-z (2023).
554 25 Cao, Y., Namkung, Y. & Laporte, S. A. Methods to Monitor the Trafficking of beta-
555   Arrestin/G Protein-Coupled Receptor Complexes Using Enhanced Bystander BRET.
556   *Methods Mol Biol* **1957**, 59-68, doi:10.1007/978-1-4939-9158-7_3 (2019).
557 26 Namkung, Y. *et al.* Monitoring G protein-coupled receptor and beta-arrestin trafficking in
558   live cells using enhanced bystander BRET. *Nat Commun* **7**, 12178,
559   doi:10.1038/ncomms12178 (2016).
560 27 Ballister, E. R., Rodgers, J., Martial, F. & Lucas, R. J. A live cell assay of GPCR coupling
561   allows identification of optogenetic tools for controlling Go and Gi signaling. *BMC Biol* **16**,
562   10, doi:10.1186/s12915-017-0475-2 (2018).
563 28 Binkowski, B. F. *et al.* A luminescent biosensor with increased dynamic range for
564   intracellular cAMP. *ACS Chem Biol* **6**, 1193-1197, doi:10.1021/cb200248h (2011).
565 29 Jiang, L. I. *et al.* Use of a cAMP BRET sensor to characterize a novel regulation of cAMP
566   by the sphingosine 1-phosphate/G13 pathway. *J Biol Chem* **282**, 10576-10584,
567   doi:10.1074/jbc.M609695200 (2007).
568 30 Ma, Q., Ye, L., Liu, H., Shi, Y. & Zhou, N. An overview of Ca(2+) mobilization assays in
569   GPCR drug discovery. *Expert Opin Drug Discov* **12**, 511-523,
570   doi:10.1080/17460441.2017.1303473 (2017).
571 31 Kroeze, W. K. *et al.* PRESTO-Tango as an open-source resource for interrogation of the
572   druggable human GPCRome. *Nature structural & molecular biology* **22**, 362-369,
573   doi:10.1038/nsmb.3014 (2015).
574 32 Cheng, Z. *et al.* Luciferase Reporter Assay System for Deciphering GPCR Pathways.
575   *Current chemical genomics* **4**, 84-91, doi:10.2174/1875397301004010084 (2010).
576 33 Fang, Y., Li, G. & Ferrie, A. M. Non-invasive optical biosensor for assaying endogenous
577   G protein-coupled receptors in adherent cells. *J Pharmacol Toxicol Methods* **55**, 314-322,
578   doi:10.1016/j.vascn.2006.11.001 (2007).
579 34 Verdonk, E. *et al.* Cellular dielectric spectroscopy: a label-free comprehensive platform for
580   functional evaluation of endogenous receptors. *Assay Drug Dev Technol* **4**, 609-619,
581   doi:10.1089/adt.2006.4.609 (2006).
582 35 Watkins, L. R. & Orlandi, C. In vitro profiling of orphan G protein coupled receptor (GPCR)
583   constitutive activity. *Br J Pharmacol* **178**, 2963-2975, doi:10.1111/bph.15468 (2021).
584 36 Che, F. Y., Lim, J., Pan, H., Biswas, R. & Fricker, L. D. Quantitative neuropeptidomics of
585   microwave-irradiated mouse brain and pituitary. *Mol Cell Proteomics* **4**, 1391-1405,
586   doi:10.1074/mcp.T500010-MCP200 (2005).
587 37 Conklin, B. R., Farfel, Z., Lustig, K. D., Julius, D. & Bourne, H. R. Substitution of three
588   amino acids switches receptor specificity of Gq alpha to that of Gi alpha. *Nature* **363**, 274-
589   276, doi:10.1038/363274a0 (1993).
590 38 Inoue, A. *et al.* Illuminating G-Protein-Coupling Selectivity of GPCRs. *Cell* **177**, 1933-1947
591   e1925, doi:10.1016/j.cell.2019.04.044 (2019).
592 39 Barnett, M. E., Knapp, B. I. & Bidlack, J. M. Unique Pharmacological Properties of the
593   Kappa Opioid Receptor Signaling Through Galphaz as Shown with Bioluminescence

Resonance Energy Tranfer. *Mol Pharmacol* **98**, 462-474, doi:10.1124/mol.120.119404 (2020).

40   Keen, A. C. *et al.* OZITX, a pertussis toxin-like protein for occluding inhibitory G protein signalling including Galpha(z). *Commun Biol* **5**, 256, doi:10.1038/s42003-022-03191-5 (2022).

41   Dunn, H. A., Orlandi, C. & Martemyanov, K. A. Beyond the Ligand: Extracellular and Transcellular G Protein-Coupled Receptor Complexes in Physiology and Pharmacology. *Pharmacological reviews* **71**, 503-519, doi:10.1124/pr.119.018044 (2019).

42   Devane, W. A. *et al.* Isolation and structure of a brain constituent that binds to the cannabinoid receptor. *Science* **258**, 1946-1949, doi:10.1126/science.1470919 (1992).

43   Kojima, M. *et al.* Ghrelin is a growth-hormone-releasing acylated peptide from stomach. *Nature* **402**, 656-660, doi:10.1038/45230 (1999).

44   Staleva, L. & Orlow, S. J. Ocular albinism 1 protein: trafficking and function when expressed in Saccharomyces cerevisiae. *Exp Eye Res* **82**, 311-318, doi:10.1016/j.exer.2005.07.003 (2006).

45   Tatemoto, K. *et al.* Isolation and characterization of a novel endogenous peptide ligand for the human APJ receptor. *Biochem Biophys Res Commun* **251**, 471-476, doi:10.1006/bbrc.1998.9489 (1998).

46   Mechoulam, R. *et al.* Identification of an endogenous 2-monoglyceride, present in canine gut, that binds to cannabinoid receptors. *Biochem Pharmacol* **50**, 83-90, doi:10.1016/0006-2952(95)00109-d (1995).

47   Franchini, L. & Orlandi, C. Deorphanization of G Protein Coupled Receptors (GPCRs): a historical perspective. *Mol Pharmacol*, doi:10.1124/molpharm.124.000900 (2024).

48   Doi, M. *et al.* Gpr176 is a Gz-linked orphan G-protein-coupled receptor that sets the pace of circadian behaviour. *Nat Commun* **7**, 10583, doi:10.1038/ncomms10583 (2016).

49   Smith, N. J. Drug Discovery Opportunities at the Endothelin B Receptor-Related Orphan G Protein-Coupled Receptors, GPR37 and GPR37L1. *Front Pharmacol* **6**, 275, doi:10.3389/fphar.2015.00275 (2015).

50   Meyer, R. C., Giddens, M. M., Schaefer, S. A. & Hall, R. A. GPR37 and GPR37L1 are receptors for the neuroprotective and glioprotective factors prosaptide and prosaposin. *Proceedings of the National Academy of Sciences of the United States of America* **110**, 9529-9534, doi:10.1073/pnas.1219004110 (2013).

51   Pandy-Szekeres, G. *et al.* The G protein database, GproteinDb. *Nucleic Acids Res* **50**, D518-D525, doi:10.1093/nar/gkab852 (2022).

52   Pandy-Szekeres, G. *et al.* GproteinDb in 2024: new G protein-GPCR couplings, AlphaFold2-multimer models and interface interactions. *Nucleic Acids Res* **52**, D466-D475, doi:10.1093/nar/gkad1089 (2024).

53   Jeffrey, J. J., Ehlich, L. S. & Roswit, W. T. Serotonin: an inducer of collagenase in myometrial smooth muscle cells. *J Cell Physiol* **146**, 399-406, doi:10.1002/jcp.1041460310 (1991).

54   Sakakibara, S. *et al.* Identification of lysophosphatidic acid in serum as a factor that promotes epithelial apical junctional complex organization. *J Biol Chem* **298**, 102426, doi:10.1016/j.jbc.2022.102426 (2022).

55   Saucier, C., Morris, S. J. & Albert, P. R. Endogenous serotonin-2A and -2C receptors in Balb/c-3T3 cells revealed in serotonin-free medium: desensitization and down-regulation by serotonin. *Biochem Pharmacol* **56**, 1347-1357, doi:10.1016/s0006-2952(98)00244-5 (1998).

56   Lu, S., Jang, W., Inoue, A. & Lambert, N. A. Constitutive G protein coupling profiles of understudied orphan GPCRs. *PLoS One* **16**, e0247743, doi:10.1371/journal.pone.0247743 (2021).

19

644 57 Schihada, H., Shekhani, R. & Schulte, G. Quantitative assessment of constitutive G
645   protein-coupled receptor activity with BRET-based G protein biosensors. *Sci Signal* **14**,
646   eabf1653, doi:10.1126/scisignal.abf1653 (2021).
647 58 Yamaguchi, Y. *et al.* Nmu/Nms/Gpr176 Triple-Deficient Mice Show Enhanced Light-
648   Resetting of Circadian Locomotor Activity. *Biol Pharm Bull* **45**, 1172-1179,
649   doi:10.1248/bpb.b22-00260 (2022).
650 59 Nakagawa, S., Nguyen Pham, K. T., Shao, X. & Doi, M. Time-Restricted G-Protein
651   Signaling Pathways via GPR176, G(z), and RGS16 Set the Pace of the Master Circadian
652   Clock in the Suprachiasmatic Nucleus. *Int J Mol Sci* **21**, doi:10.3390/ijms21145055 (2020).
653 60 De Smet, V. *et al.* Orphan receptor GPR176 in hepatic stellate cells exerts a profibrotic
654   role in chronic liver disease. *JHEP Rep* **6**, 101036, doi:10.1016/j.jhepr.2024.101036
655   (2024).
656 61 Fu, W., Franchini, L. & Orlandi, C. Comprehensive Spatial Profile of the Orphan G Protein
657   Coupled Receptor GPRC5B Expression in Mouse Brain. *Front Neurosci* **16**, 891544,
658   doi:10.3389/fnins.2022.891544 (2022).
659 62 Zhang, Q., Bang, S., Chandra, S. & Ji, R. R. Inflammation and Infection in Pain and the
660   Role of GPR37. *Int J Mol Sci* **23**, doi:10.3390/ijms232214426 (2022).
661 63 Meyer, R. C., Giddens, M. M., Coleman, B. M. & Hall, R. A. The protective role of
662   prosaposin and its receptors in the nervous system. *Brain Res* **1585**, 1-12,
663   doi:10.1016/j.brainres.2014.08.022 (2014).
664 64 Bolinger, A. A., Frazier, A., La, J. H., Allen, J. A. & Zhou, J. Orphan G Protein-Coupled
665   Receptor GPR37 as an Emerging Therapeutic Target. *ACS Chem Neurosci* **14**, 3318-
666   3334, doi:10.1021/acschemneuro.3c00479 (2023).
667 65 Bang, S. *et al.* GPR37 regulates macrophage phagocytosis and resolution of inflammatory
668   pain. *J Clin Invest* **128**, 3568-3582, doi:10.1172/JCI99888 (2018).
669 66 Liu, B. *et al.* Glio- and neuro-protection by prosaposin is mediated by orphan G-protein
670   coupled receptors GPR37L1 and GPR37. *Glia* **66**, 2414-2426, doi:10.1002/glia.23480
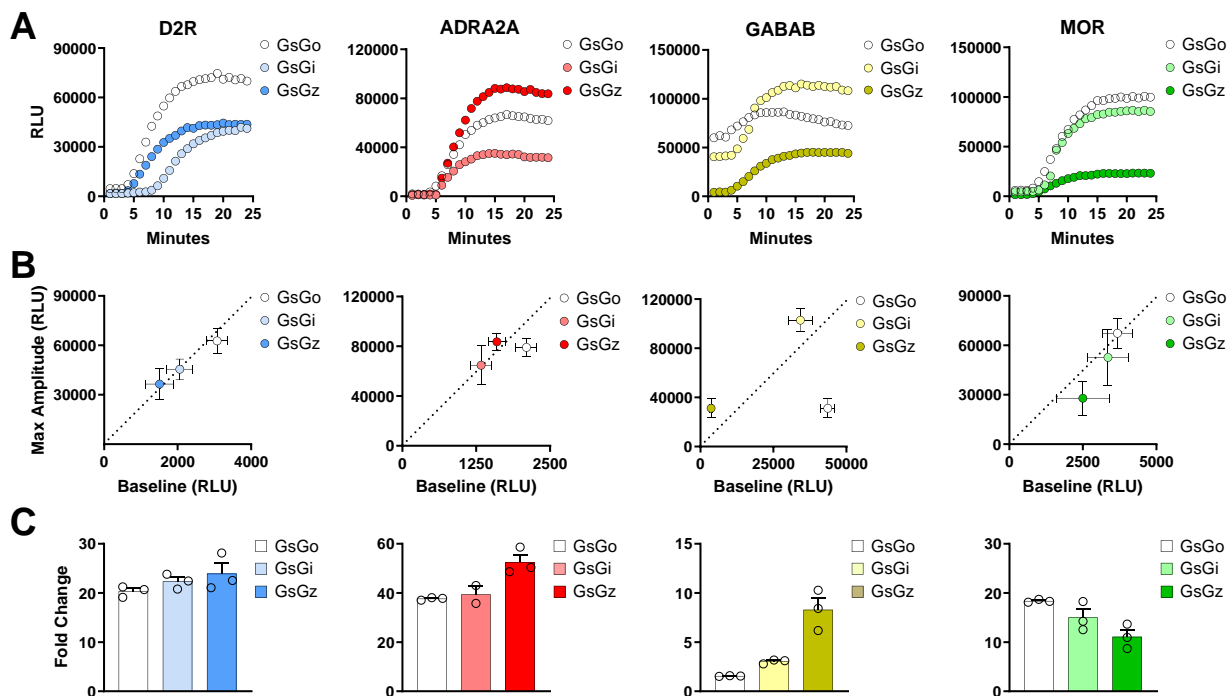671   (2018).

672

Figure 1

Figure 1. Real-time activation of Gs-based chimeras by $G_{i/o/z}$-coupled receptors. (**A**) Representative kinetics of cAMP accumulation in response to agonist stimulation of indicated GPCRs using 10 µM dopamine, 10 µM clonidine, 10 µM GABA, and 1 µM DAMGO, respectively. (**B**) Correlation between maximal amplitude and basal signal for each receptor co-expressed with indicated G protein chimeras. (**C**) Fold change calculated as the ratio of maximal amplitude over baseline reported in panel **B**. Data are shown as means ± SEM. N=3 independent replicates.

Figure 2
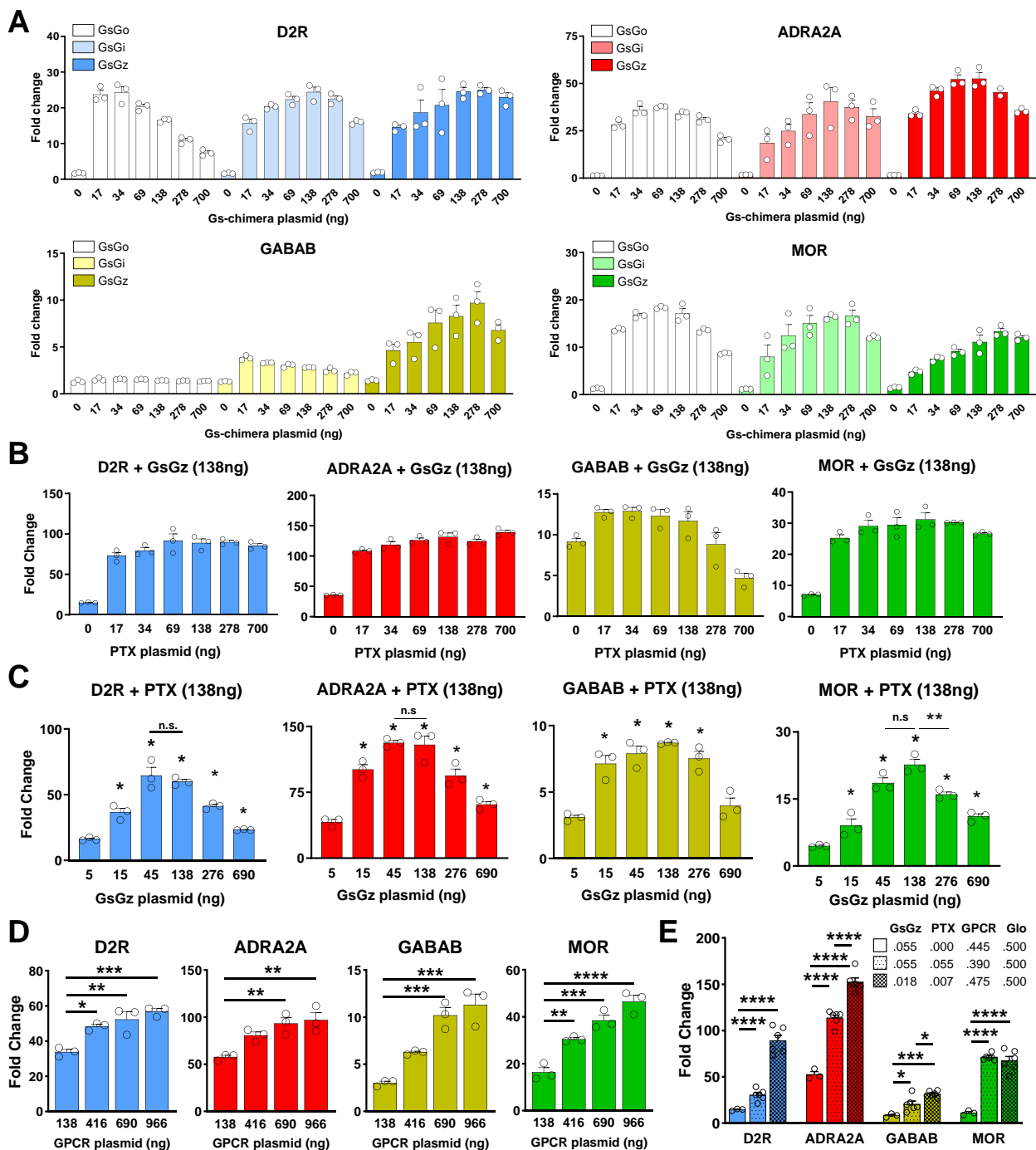
Figure 2. Optimization of transfection ratios between G$_z$ESTY components. (**A**) Activation of indicated GPCRs with increasing amount of transfected Gs-based chimeras. (**B**) GPCR activation with the introduction of increasing concentrations of PTX-S1 subunit to eliminate the inhibition of adenylyl cyclase by endogenous G$_{i/o}$ proteins. (**C**) GPCR activation in the presence of increasing amount of transfected GsGz plasmid. (**D**) Signal fold change with titration of each transfected receptor. (**E**) Fold-change comparison between standard transfection ratio and optimized ratio 50:47.5:1.8:0.7 (GloSensor:GPCR:GsGz:PTX). The data shown represent the average of 3-6 independent experiments (one-way ANOVA with Dunnett's multiple comparisons test, *p < .05; **p < .01; ***p < .001; ****p < .0001). Data are shown as means ± SEM.
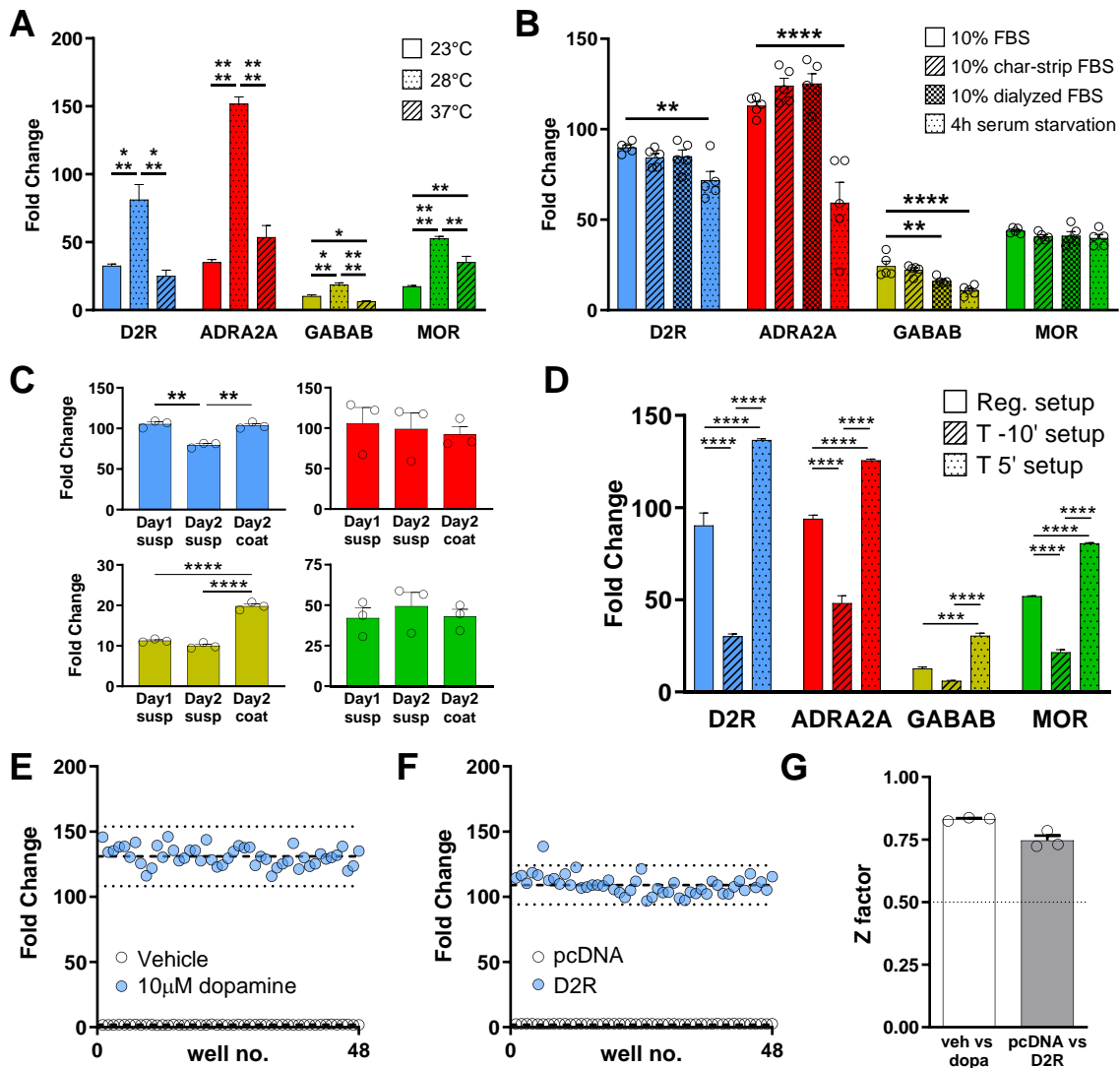
Figure 3

Figure 3. G$_z$ESTY protocol optimization and Z factor calculation. (**A**) Assay temperature influences assay sensitivity. Assays performed at 28°C give a significantly higher signal. (**B**) FBS removal (4h serum starvation), use of charcoal-stripped FBS, or use of dialyzed FBS did not improve the assay signal. (**C**) Assays performed with cells in adhesion show a signal improvement for GABAB receptor but not for D2R, ADRA2A, and MOR. (**D**) Co-treatment with IBMX (T 5' setup) significantly increases the signal with each of the four GPCRs. Data shown represent the average of 3-5 independent experiments (one-way ANOVA with Dunnett's multiple comparisons test, *p < .05; **p < .01; ***p < .001; ****p < .0001). Data are shown as means ± SEM. (**E**) Cells transiently transfected with D2R were treated with either 10 µM dopamine or vehicle. Dashed lines represent the means of the fold change. Dotted lines display three standard deviations from the mean of each data set. (**F**) Cells transfected with indicated plasmids were treated with 10 µM dopamine. Dashed lines represent the means of the fold change for cells expressing D2R or cells not expressing exogenous GPCRs (pcDNA, control). (**G**) Z factor calculation. Dotted lines indicate the threshold for robust assays. Data shown in panels **E** and **F** are representative of three independent experiments quantified in panel **G** as means ± SEM.
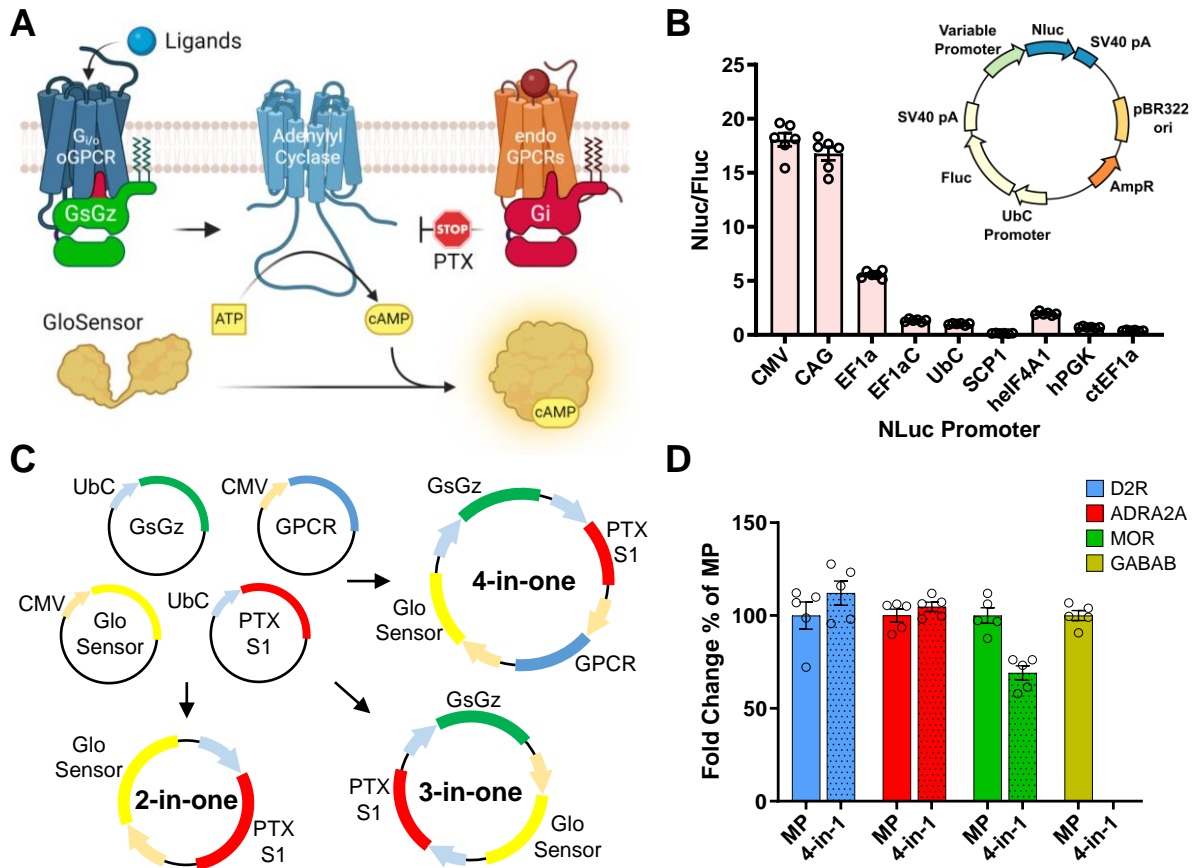
Figure 4

Figure 4. All-in-one G$_z$ESTY plasmids. (**A**) Schematics of G$_z$ESTY and each of its components. (**B**) Promoter efficiency estimation calculated as Nluc luminescence normalized over firefly luminescence signal in HEK293 cells transfected with a plasmid encoding nanoluc under the control of each of the indicated promoters and firefly under the control of UbC promoter. N=6 (**C**) Maps of the all-in-one plasmids generated. (**D**) Assay comparison in cells transiently transfected with four single plasmids or with each of the 4-in-one plasmids encoding each indicated GPCR. Data are shown as means ± SEM; N=5.
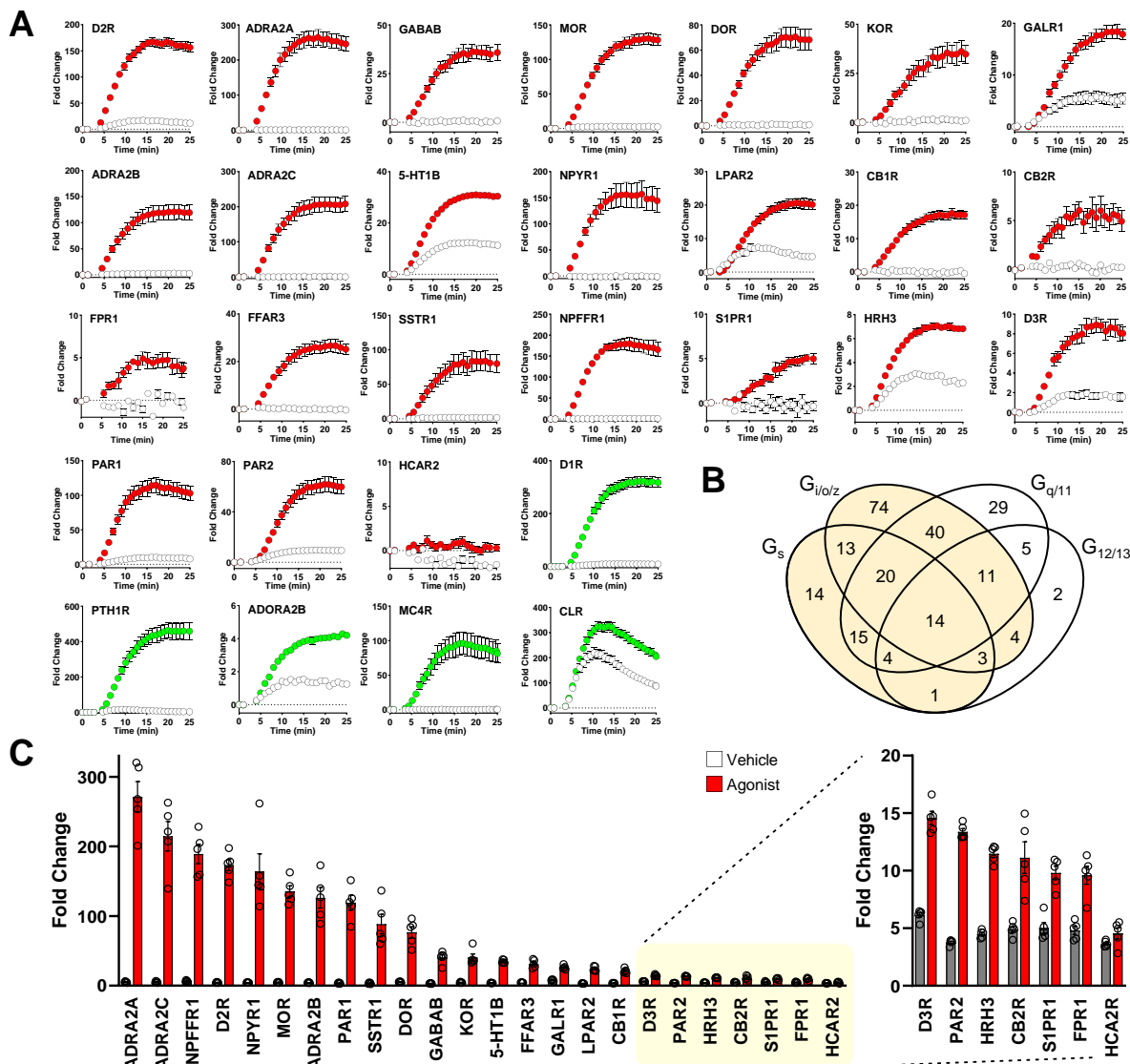
Figure 5

A

B

C

Figure 5. G$_z$ESTY applied to a battery of ligand-activated GPCRs. (**A**) Real-time analysis of ligand-mediated activation of a battery of G$_{i/o/z}$-PCRs (red) and G$_s$-PCR (green) in cells co-transfected with indicated receptors and the 3-in-one G$_z$ESTY plasmid in the presence of 50 µM IBMX. Cells transfected only with the 3-in-one plasmid served as control (white). The following agonists were applied at 4 minutes: 10 µM dopamine (D2R, D1R), 100 µM clonidine (ADRA2A, ADRA2B, ADRA2C), 10 µM GABA (GABABR), 10 µM DAMGO (MOR), 1 µM SNC-80 (DOR), 10 µM salvinorin A (KOR), 10 µM human galanin (1-30) (GAL1R), 100 µM serotonin (5-HT1B), 10 µM human neuropeptide Y (13-36) (NPYR1), 10 µM lysophosphatidic acid (LPAR2), 10 µM 2-arachidonoyl glycerol (CB1R, CB2R), 10 µM N-formyl-met-leu-phe (FPR1), 1 mM isobutyric acid (FFAR3), 10 µM somatostatin 14 (SSTR1), 10 µM neuropeptide FF (NPFFR1), 10 µM SEW2871 (S1PR1), 10 µM histamine (HRH3), 10 µM quinpirole (D3R), 10 µM TFLLR (PAR1), 10 µM SLIGKV (PAR2), 10 µM MK-6892 (HCA2R), 1 µM teriparatide PTH (PTH1R), 10 µM AB-MECA (ADORA2B), 10 µM NDP-α-MSH (MC4R), and 10 µM CGRP (CLR). Data are shown as means ± SEM; N=5. (**B**) GPCRs that couple to G$_s$ and/or G$_{i/o/z}$ and can potentially be detected by GZESTY are highlighted and include 213 out of 249 total ligand-activated GPCRs (86%) (adapted from GPRCdb.org). (**C**) Quantification of agonist-induced activity for 24 G$_{i/o/z}$-coupled GPCRs. On the right, the response to agonist of the last seven GPCRs is also reported with a different scale. Data are shown as means ± SEM of the fold change obtained; N=5.
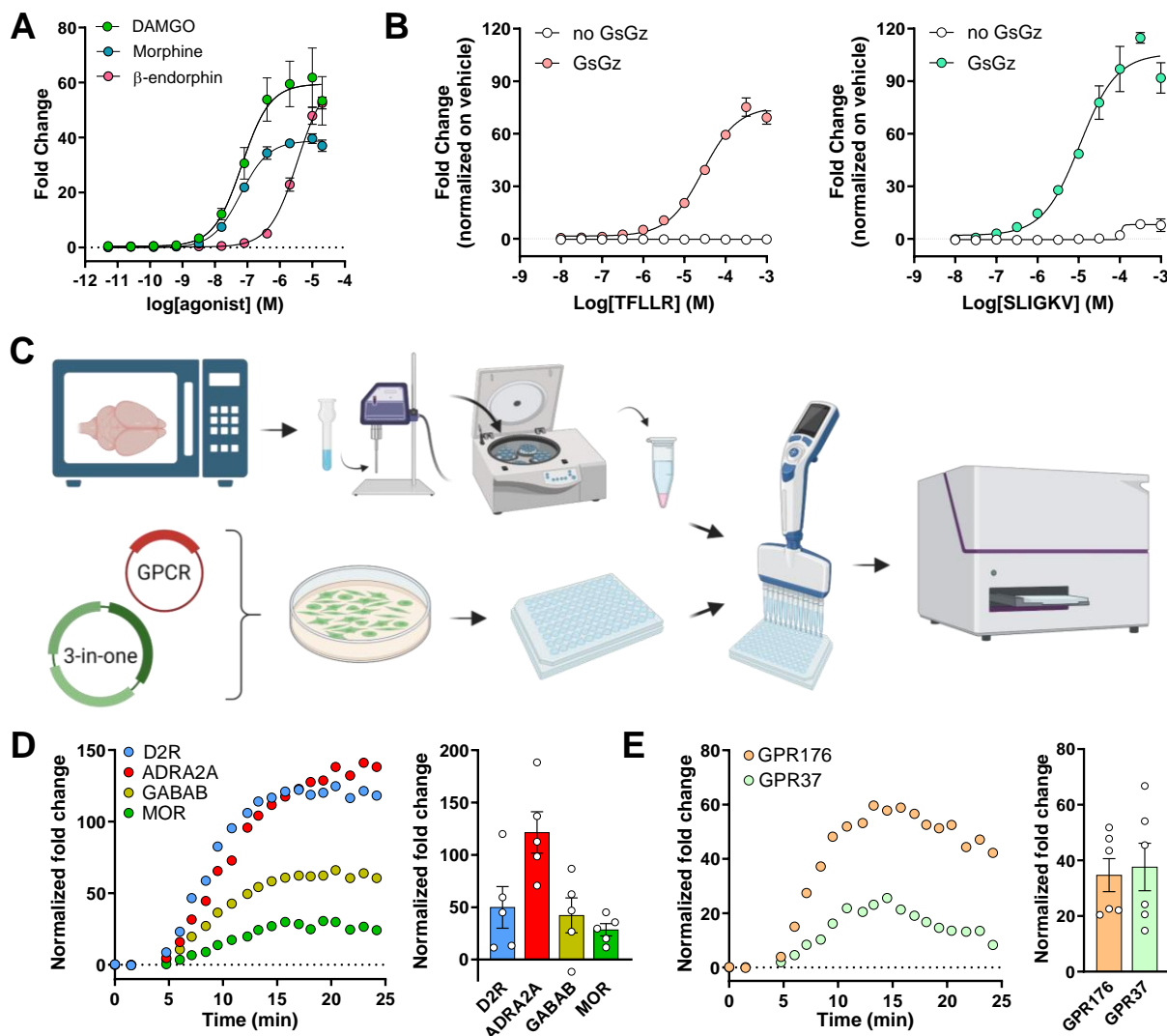
Figure 6

Figure 6. G$_z$ESTY applications. (**A**) Concentration-response curves obtained for MOR stimulated with DAMGO, morphine, or β-endorphin. Data are shown as means ± SEM; N=3. (**B**) Concentration-response curves of endogenously expressed PAR1 activated with a selective agonist peptide TFLLR (left) or PAR2 activated with selective agonist peptide SLIGKV (right) in cells transfected only with the 3-in-one plasmid. Control cells were transfected with a 2-in-one plasmid not expressing GsGz chimera. Data are shown as means ± SEM; N=3. (**C**) Schematics of G$_z$ESTY application to test ligand presence in mouse brain extract. Mouse brains were isolated after 10'' of microwave exposure to preserve peptides and small molecules from degradation. Brain homogenates were sonicated, and debris and insoluble materials were separated by centrifugation. Supernatant was then applied to cells transfected with G$_z$ESTY and resuspended in 96-well plates. cAMP levels were measured before and after brain extract application for a total of 25 minutes (created with BioRender). (**D**) Crude brain extract application induces activation of D2R, ADRA2A, MOR, and GABAB receptors. Representative traces (left) and quantification of 5 independent experiments (right) indicate the presence of endogenous ligands in the brain extract. Data are shown as means ± SEM; N=5. (**E**) Representative traces (left) and quantification (right) indicating the activation of GPR176 and GPR37 by crude brain extract application. Data are shown as means ± SEM; N=6.